UDK 539.3

CONTACT STRENGTH OF TWO ELASTIC HALF-SPACES WITH A CIRCULAR RECESS

B. MONASTYRSKYY [1], *A. KACZYŃSKI* [2]

[1] *Pidstryhach Institute for Applied Problems of Mechanics and Mathematics, NASU, Lviv;*
[2] *Faculty of Mathematics and Information Science,Warsaw University of Technology*

The paper presents the analysis of the stress-and-strain state of a contacting couple consisting of two isotropic semi-infinite solids one of which has a small surface recess. Based on the classical criteria of fracture, namely the criterion of maximal principle stresses and criterion of maximal shear stresses, the regions of the most possible crack initial and plastic zones formation have been found. The brittle cracking can be induced by both tensile and compressive stresses arising at the interface. For some shape of the recess, considered as an example, the analysis reveals that the fracture starts from the contacting solids boundary.

Key words: *contact problem, conforming boundaries, local fault of contact, contact strength, criterion of maximal principle stresses, criterion of maximal shear stresses.*

The paper is a continuation of our previous study [1] concerning the problem of frictionless contact of two compressed elastic half-spaces provided one of them possesses a small circular surface recess. The aim of this work is to examine the behavior of the contacting solids from the point of view of contact fracture mechanics. Strength analysis is carried out by using the closed-form solution obtained in [1] for a special form of the recess and by employing some classical fracture criteria.

The knowledge of the solutions (especially analytical ones) to contact problems serves as a ground for the investigation of strength, durability and fatigue of contacting couples. The majority of works of contacting joints on strength utilizes the solutions obtained within the framework of a theory of Hertzian contact. But these solutions are useful only for contact of solids with mismatching surfaces (see a classification by Johnson [2]). Extensive literature on the subject is discussed in the book by Kolesnikov and Morozov [3]. On the contrary, the contact interaction of bodies with conformable surfaces has been investigated much less. The contact strength of solids with recesses has been analyzed in [4]. Approaches employing this kind of interaction take into account the existence of imperfections (recesses, pits, protrusions, concavities, etc.) of surfaces related to their small deviations from a flat onto local parts. Such perturbations lead to the local absence of contact, so the intercontact gaps are created. The problem under study belongs to the class of non-classical contact problems involving contact interactions of solids with conformed surfaces.

Description of the problem. This paper deals with an axisymmetric problem of elastic contact of two different isotropic elastic semi-infinite solids one of which (denoted by 1, see Fig. 1) possesses a local surface recess occupying a circular region of radius b. In the cylindrical co-ordinate system, introduced in such a way as it is shown in Fig. 1, the profile of the surface recess is described by a given function $f(r)$.

The solids are pressed to each other by normal uniform forces p at infinity. Since the initial relieves of the surfaces are mismatched, their contact is imperfect and during the interaction an intersurface gap is formed. It is assumed that the region of the gap is circular of an unknown a priori radius a.

Corresponding author: B. MONASTYRSKYY, e-mail: bmonast@iapmm.lviv.ua

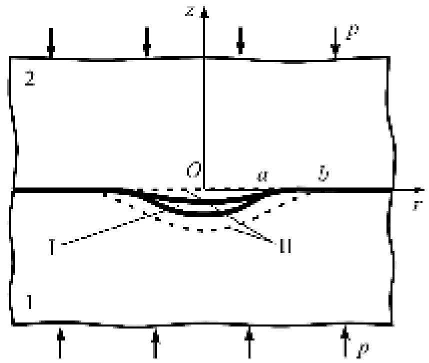

Fig. 1. Contact of two half-spaces with allowance for intersurface gap.
I – intersurface gap;
II – initial relief of boundaries.

A method to solve the above problem was presented in [1]. It represents the displacements and stresses in the contacting couple through the unknown function of the interface gap height $h(r) = f(r) + u_z^{(2)}(r,0) - u_z^{(1)}(r,0)$, $r < a$. It was shown that the perturbed problem with the following boundary conditions

$$z = \pm\infty: \quad \sigma_{zz}^{(i)} = 0, \ \sigma_{rz}^{(i)} = 0, \tag{1}$$

$$z = 0: \quad \sigma_{rz}^{(i)} = 0, \quad 0 < r < \infty, \tag{2}$$

$$\sigma_{zz}^{(1)} = \sigma_{zz}^{(2)}, \quad 0 < r < \infty, \tag{3}$$

$$\sigma_{zz}^{(2)} = p, \quad 0 < r < a, \tag{4}$$

$$u_z^{(1)} - u_z^{(2)} = f(r), \quad a < r < \infty, \tag{5}$$

can be reduced to the dual integral equations for the Hankel transform of the gap height $H(\xi) = \int_0^\infty \rho\, h(\rho)\, J_0(\xi\rho)\, d\rho$:

$$\int_0^\infty \xi^2 H(\xi)\, J_0(\xi r)\, d\xi = -\frac{p}{M} + \int_0^\infty \xi^2 F(\xi)\, J_0(\xi r)\, d\xi, \quad 0 < r < a, \tag{6}$$

$$\int_0^\infty \xi H(\xi)\, J_0(\xi r)\, d\xi = 0, \quad a < r < \infty \cdot \tag{7}$$

Notation here is the same as in [1]. In particular, $F(\xi) = \int_0^\infty \rho\, f(\rho)\, J_0(\xi\rho)\, d\rho$, $J_k(\cdot)$ are the Bessel functions of the first kind of order *k*, $m_i = \mu_i/(1-\nu_i)$, $M = \dfrac{m_1 m_2}{m_1 + m_2}$, and μ_i, ν_i stand for shear modulus and Poisson's ratio of the body denoted by $i = 1, 2$.

The solution to equations (6)–(7) can be determined from the sequence of the relations:

$$H(\xi) = \xi^{-1} \int_0^a \gamma(\rho) \sin \xi\rho\, d\rho, \tag{8}$$

$$\gamma(r) = \frac{2}{\pi} \int_0^r \rho\, g(\rho) \Big/ \sqrt{r^2 - \rho^2}\, d\rho, \tag{9}$$

where

$$g(r) = -\frac{p}{M} + \int_0^\infty \xi^2 F(\xi)\, J_0(\xi r)\, d\xi.$$

Now we recall the formulas for non-vanishing components of stress tensor:

$$\frac{\sigma_{rz}^{(i)}(r,z)}{M} = z \int_0^\infty \xi^3 (F(\xi) - H(\xi)) e^{-\xi|z|} J_1(\xi r)\, d\xi, \tag{10}$$

$$\frac{\sigma_{zz}^{(i)}(r,z)}{M} = \int_0^\infty \xi^2 \left[(1 + \xi|z|)(F(\xi) - H(\xi))\right] e^{-\xi|z|} J_0(\xi r)\, d\xi, \tag{11}$$

$$\frac{\sigma_{rr}^{(i)}(r,z)}{M} = \int_0^\infty \xi^2 \left[(1 - \xi|z|)(F(\xi) - H(\xi))\right] e^{-\xi|z|} J_0(\xi r)\, d\xi -$$

$$-\int_0^\infty \xi\left[(1-2\nu_i-\xi|z|)(F(\xi)-H(\xi))\right]e^{-\xi|z|}\frac{J_1(\xi r)}{r}d\xi, \tag{12}$$

$$\frac{\sigma_{\theta\theta}^{(i)}(r,z)}{M}=2\nu_i\int_0^\infty \xi^2(F(\xi)-H(\xi))e^{-\xi|z|}J_0(\xi r)d\xi+$$
$$+\int_0^\infty \xi\left[(1-2\nu_i-\xi|z|)(F(\xi)-H(\xi))\right]e^{-\xi|z|}\frac{J_1(\xi r)}{r}d\xi. \tag{13}$$

To complete the problem solution, it is necessary to determine the radius of the gap a from the condition of smooth closing of the gap [1]:

$$\gamma(a)=0. \tag{14}$$

Now it is further assumed that the shape of the initial recess is given as

$$f(r)=h_0(1-r^2/b^2)^{3/2} \quad (0\le r\le b,\ h_0=f(0)=b). \tag{15}$$

For this case, the Hankel transform $F(\xi)$ of $f(r)$ is [5]

$$F(\xi)=h_0b^2 2^{3/2}\Gamma(5/2)(\xi b)^{-(5/2)}J_{5/2}(\xi b). \tag{16}$$

Then from (9) it is found that

$$\gamma(r)=-2/\pi[p/M-3\pi h_0/4b(1-r^2/b^2)]r \tag{17}$$

and equation (14) yields the following value of the radius of the gap *a*:

$$a=b\sqrt{1-4pb/(3\pi M h_0)}\ . \tag{18}$$

From this expression we can easily find the threshold value of external pressure for which the gap is completely closed (i.e. *a*=0): $p_{\text{threshold}}=M3\pi h_0/4b$.

Moreover, using the results expressed by equations (16)–(18) and (8) we can determine the stress distribution given by (10)–(13). After calculating the corresponding integrals [5, 6] the complete stress field in elementary functions is obtained in the following form:

$$\frac{\sigma_{rz}^{(i)}(r,z)}{M}=z\frac{h_0}{b^3}\left(-3b^2 Int_1(r,z,b)+9Int_2(r,z,b)+3a^2 Int_1(r,z,a)-9Int_2(r,z,a)\right), \tag{19}$$

$$\frac{\sigma_{zz}^{(i)}(r,z)}{M}=$$
$$=-p+\frac{h_0}{b^3}\Big(-3b^2Int_3(r,z,b)+9Int_4(r,z,b)+z\left(-3b^2Int_5(r,z,b)+9Int_6(r,z,b)\right)+ \tag{20}$$
$$+3a^2Int_3(r,z,a)-9Int_4(r,z,a)+z\left(3a^2Int_5(r,z,a)-9Int_6(r,z,a)\right)\Big),$$

$$\frac{\sigma_{rr}^{(i)}(r,z)}{M}=\frac{h_0}{b^3}\Big((1-2\nu_i)\left(-3b^2Int_7(r,z,b)+9Int_8(r,z,b)\right)+$$
$$+z\left(-3b^2Int_9(r,z,b)+9Int_{10}(r,z,b)\right)+(1-2\nu_i)\left(3a^2Int_7(r,z,a)-9Int_8(r,z,a)\right)+$$
$$+z\left(3a^2Int_9(r,z,a)-9Int_{10}(r,z,a)\right)\Big)+\frac{h_0}{b^3}\Big(-3b^2Int_3(r,z,b)+9Int_4(r,z,b)+ \tag{21}$$
$$+z\left(-3b^2Int_5(r,z,b)+9Int_6(r,z,b)\right)+3a^2Int_3(r,z,a)-9Int_4(r,z,a)+$$
$$+z\left(3a^2Int_5(r,z,a)-9Int_6(r,z,a)\right)\Big),$$

$$\frac{\sigma_{\theta\theta}^{(i)}(r,z)}{M}=\frac{h_0}{b^3}\Big((1-2\nu_i)\Big(-3b^2\,Int_7(r,z,b)+9Int_8(r,z,b)\Big)+$$
$$+z\Big(-3b^2\,Int_9(r,z,b)+9Int_{10}(r,z,b)\Big)+(1-2\nu_i)\Big(3a^2\,Int_7(r,z,a)-9Int_8(r,z,a)\Big)+$$
$$+z\Big(3a^2\,Int_9(r,z,a)-9Int_{10}(r,z,a)\Big)\Big)+ \qquad (22)$$
$$+2\nu_i\frac{h_0}{b^3}\Big(-3b^2\,Int_3(r,z,b)+9Int_4(r,z,b)+3a^2\,Int_3(r,z,a)-9Int_4(r,z,a)\Big),$$

where $Int_k(r,z,b)$ ($k=\overline{1,10}$) stands for the integrals given by formulas:

$$Int_1(r,z,b)=\int_0^\infty e^{-\xi z}\sin(\xi b)J_1(\xi r)d\xi=$$
$$=\begin{cases}\dfrac{b\cos\left(\frac{1}{2}\mathrm{arctg}\left(\frac{2zb}{z^2-b^2+r^2}\right)\right)-z\sin\left(\frac{1}{2}\mathrm{arctg}\left(\frac{2zb}{z^2-b^2+r^2}\right)\right)}{r\sqrt[4]{(z^2-b^2+r^2)^2+(2zb)^2}}, & z\neq 0;\\ 0, \quad z=0, & r\le b;\\ \dfrac{b}{r\sqrt{r^2-b^2}}, \quad z=0, & r>b;\end{cases}$$

$$Int_2(r,z,b)=\int_0^\infty e^{-\xi z}\frac{\sin(\xi b)-\xi b\cos(\xi b)}{\xi^2}J_1(\xi r)d\xi=$$
$$=\begin{cases}\displaystyle\int_0^b \beta\,Int_1(r,z,\beta)d\beta, & z\neq 0;\\ \dfrac{\pi r}{4}, \quad z=0, & r\le b;\\ -\dfrac{b\sqrt{r^2-b^2}}{2r}+\dfrac{r}{2}\arcsin\left(\dfrac{b}{r}\right), \quad z=0, & r>b;\end{cases}$$

$$Int_3(r,z,b)=\int_0^\infty e^{-\xi z}\frac{\sin(\xi b)}{\xi}J_0(\xi r)d\xi=\begin{cases}\arcsin\left(\dfrac{2b}{\sqrt{(b+r)^2+z^2}+\sqrt{(b-r)^2+z^2}}\right), & z\neq 0;\\ \dfrac{\pi}{2}, \quad z=0, & r\le b;\\ \arcsin\left(\dfrac{b}{r}\right), \quad z=0, & r>b;\end{cases}$$

$$Int_4(r,z,b)=\int_0^\infty e^{-\xi z}\frac{\sin(\xi b)-\xi b\cos(\xi b)}{\xi^3}J_0(\xi r)d\xi=$$

$$
=\begin{cases}
\int_0^b \beta Int_3(r,z,\beta)d\beta, & z\neq 0;\\
\dfrac{\pi(2b^2-r^2)}{8}, & z=0,\quad r\le b;\\
\dfrac{1}{4}\left(b\sqrt{r^2-b^2}+(2b^2-r^2)\arcsin\left(\dfrac{b}{r}\right)\right), & z=0,\ r>b;
\end{cases}
$$

$$
Int_5(r,z,b)=\int_0^\infty \mathrm{e}^{-\xi z}\sin(\xi b)J_0(\xi r)d\xi=
$$

$$
=\begin{cases}
\dfrac{2bz}{\sqrt{\left(\sqrt{(b+r)^2+z^2}+\sqrt{(b-r)^2+z^2}\right)^2-b^2}\sqrt{(b+r)^2+z^2}\sqrt{(b-r)^2+z^2}}, & z\neq 0;\\
\dfrac{1}{\sqrt{b^2-r^2}}, & z=0,\quad r<b;\\
0, & z=0,\quad r>b;
\end{cases}
$$

$$
Int_6(r,z,b)=\int_0^\infty \mathrm{e}^{-\xi z}\frac{\sin(\xi b)-\xi b\cos(\xi b)}{\xi^2}J_0(\xi r)d\xi=\begin{cases}
\int_0^b \beta Int_5(r,z,\beta)d\beta, & z\neq 0;\\
\sqrt{b^2-r^2}, & z=0,\quad r\le b;\\
0, & z=0,\quad r>b;
\end{cases}
$$

$$
Int_7(r,z,b)=\int_0^\infty \mathrm{e}^{-\xi z}\frac{\sin(\xi b)}{\xi^2}\frac{J_1(\xi r)}{r}d\xi=
$$

$$
=\begin{cases}
\dfrac{1}{r^2}\left(-zb+\dfrac{1}{2\sqrt{2}}\left(z\sqrt{\sqrt{(z^2-b^2+r^2)^2+4z^2b^2}-(z^2-b^2+r^2)}+\right.\right.\\
\qquad\left.\left.+b\sqrt{\sqrt{(z^2-b^2+r^2)^2+4z^2b^2}+(z^2-b^2+r^2)}\right)\right)+\\
\qquad+\dfrac{1}{2}\operatorname{arctg}\left(\dfrac{\sqrt{2}b+\sqrt{\sqrt{(z^2-b^2+r^2)^2+4z^2b^2}-(z^2-b^2+r^2)}}{\sqrt{2}z+\sqrt{\sqrt{(z^2-b^2+r^2)^2+4z^2b^2}+(z^2-b^2+r^2)}}\right), & z\neq 0;\\
\dfrac{\pi}{4}, & z=0,\quad r<b;\\
\dfrac{b}{2r^2}\sqrt{r^2-b^2}+\dfrac{1}{2}\operatorname{arctg}\left(\dfrac{b}{\sqrt{r^2-b^2}}\right), & z=0,\quad r>b;
\end{cases}
$$

$$
Int_8(r,z,b)=\int_0^\infty \mathrm{e}^{-\xi z}\frac{\sin(\xi b)-\xi b\cos(\xi b)}{\xi^4}\frac{J_1(\xi r)}{r}d\xi=
$$

$$
= \begin{cases} \int_0^b \beta Int_7(r,z,\beta) d\beta, \quad z \neq 0; \\ \dfrac{\pi(4b^2 - r^2)}{32}, \qquad z = 0, \quad r \le b; \\ \dfrac{1}{16r^2}\left(b(2b^2 + r^2)\sqrt{r^2 - b^2} + (4b^2r^2 - r^4)\arcsin\left(\dfrac{b}{r}\right)\right), \quad z = 0, \ r > b; \end{cases}
$$

$$
Int_9(r,z,b) = \int_0^\infty e^{-\xi z} \frac{\sin(\xi b)}{\xi} \frac{J_1(\xi r)}{r} d\xi =
$$

$$
= \begin{cases} \dfrac{1}{r^2}\left(b - \dfrac{1}{\sqrt{2}}\sqrt{\sqrt{(z^2 - b^2 + r^2)^2 + 4z^2b^2} - (z^2 - b^2 + r^2)}\right), \quad z \neq 0; \\ \dfrac{1}{b + \sqrt{b^2 - r^2}}, \qquad z = 0, \quad r < b; \\ \dfrac{b}{r^2}, \qquad z = 0, \quad r > b; \end{cases}
$$

$$
Int_{10}(r,z,b) = \int_0^\infty e^{-\xi z} \frac{\sin(\xi b) - \xi b \cos(\xi b)}{\xi^3} \frac{J_1(\xi r)}{r} d\xi =
$$

$$
= \begin{cases} \int_0^b \beta Int_9(r,z,\beta) d\beta, \quad z \neq 0; \\ \dfrac{1}{3}\dfrac{1}{b + \sqrt{b^2 - r^2}}\left(2b^2 - r^2 + b\sqrt{b^2 - r^2}\right), \qquad z = 0, \quad r \le b; \\ \dfrac{b^3}{3r^2}, \quad z = 0, \ r > b; \end{cases}
$$

Contact strength. The obtained closed-form solution can be useful for analyzing the assessment of the contacting couple strength. To estimate the strength of a system of two mated elastic half-spaces allowing for unevenness of their boundaries, let us use the classical criteria of fracture: the criterion of maximal principle stresses and the criterion of maximal shear stresses [7].

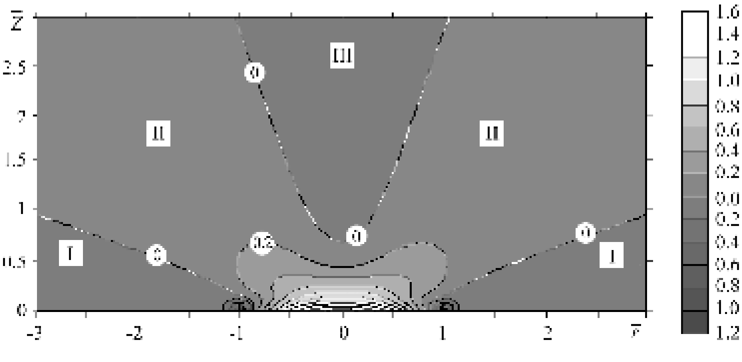

Fig. 2. Principle stress, $10^3 \cdot \bar{\sigma}_1$. I – compressive stress zone; II – tensile stress zone.

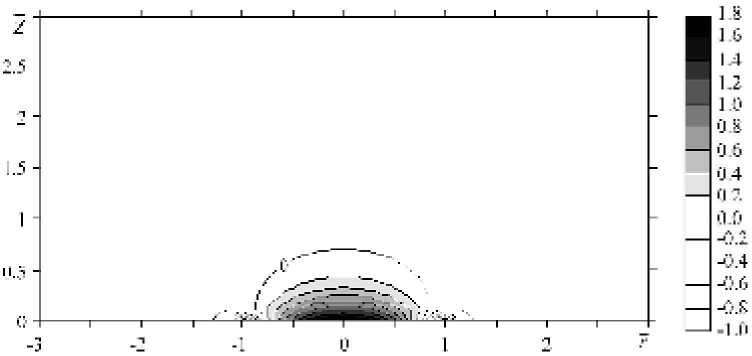

Fig. 3. Principle stress, $10^3 \cdot \bar{\sigma}_2$.

At first the stress fields in contacting bodies are analyzed. Without loss of generality the state of solid 2, regarding solid 1 as a counterpart in the contacting couple is studied. Figs. 2–4 represent the distributions of the principle stresses σ_1, σ_2, σ_3 ($\sigma_1 > \sigma_2 > \sigma_3$). The numerical analysis has been carried out for various parameters, accounting different values of external load, however the given figures show the results for the threshold external pressure $p_{\text{threshold}}$. It is motivated by the distinguished features of the stress state in this case. All the calculations were performed for the dimensionless variables: $\bar{a} = a/b,\ \bar{r} = r/b,\ \bar{z} = z/b,\ \bar{p} = p/m,\ \bar{\sigma} = \sigma/M$.

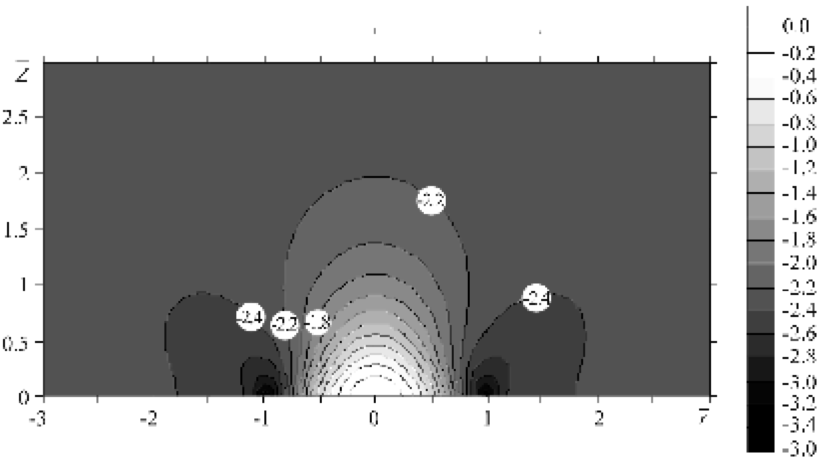

Fig. 4. Principle stress, $10^3 \cdot \bar{\sigma}_3$.

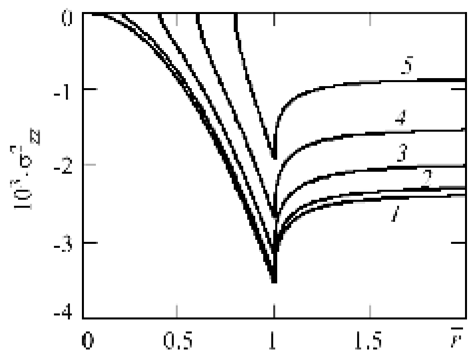

Fig. 5. Normal contact stress distribution $\bar{\sigma}_{zz}$ at the contact interface.

It is worth noting from Fig. 2 that there are zones within the contacting couple under compression where the stress σ_1 becomes tensile. This effect is caused by the existence of the local geometric excitation in one of the surfaces of conjugate solids. The stress σ_2 is negligibly small in the whole solid except of the defect vicinity. The principle stress σ_3 is compressive within the whole body. By observing principle stresses in Figs. 2–4 it is possible to see that all quantities σ_1, σ_2, σ_3 reach their extreme values at the contact interface $z = 0$. That is why let us turn to a complete analysis of stresses on this plane.

The maximal compressive stresses. Fig. 5 shows the distributions of contact normal stresses at the boundary $z = 0$ for five cases of the radius of the gap. The contact pressure reaches its maximum exactly at $\bar{r} = 1$, i.e. $r = b$. According to the criteria of maximal principle stresses it is concluded that cracking of materials caused by compressive stresses initiates in the vicinity of the recess edge.

The maximal tensile stresses. Fig. 6 demonstrates distributions of radial $\bar{\sigma}_{rr}$ and circular $\bar{\sigma}_{\theta\theta}$ stresses at the contact interface. It is seen that the stresses σ_{rr} and $\sigma_{\theta\theta}$ are: (*i*) tensile, (*ii*) constant and (*iii*) equal to each other within the gap faces, determined using the applied pressure and mechanical properties of the solids as follows:

$$\sigma_{rr}^{(i)}(r,0) = \sigma_{\theta\theta}^{(i)}(r,0) = (1+2\nu_i)\,p/2,\; 0 < r < a\,.$$

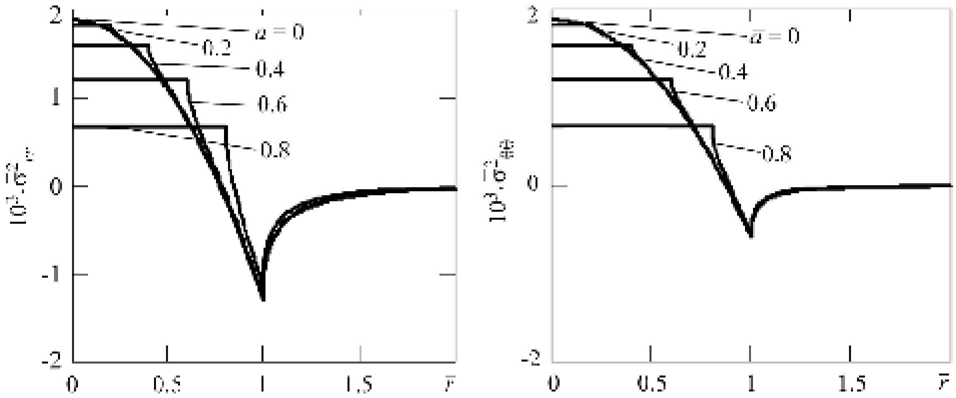

Fig. 6. Distribution of stresses $\bar{\sigma}_{rr}$ and $\bar{\sigma}_{\theta\theta}$ at the contact interface.

Thus, the cracking can be initiated by tensile stresses. The most dangerous region is the gap. Moreover, the possibilities of cracks initiating along radial and circular directions are equal.

The maximal shear stresses. The distribution of maximal shear stress τ_{max}, defined as $\tau_{max} = (\sigma_1 - \sigma_3)/2$ is presented in Fig. 7. As one can see, the extreme value arises in the interface plane $z = 0$ at $\bar{r} = 1$. So, according to the criterion of maximal shear stresses, which usually is used for assessment of plastic zones initiating, the most dangerous zone is the vicinity of the recess edge.

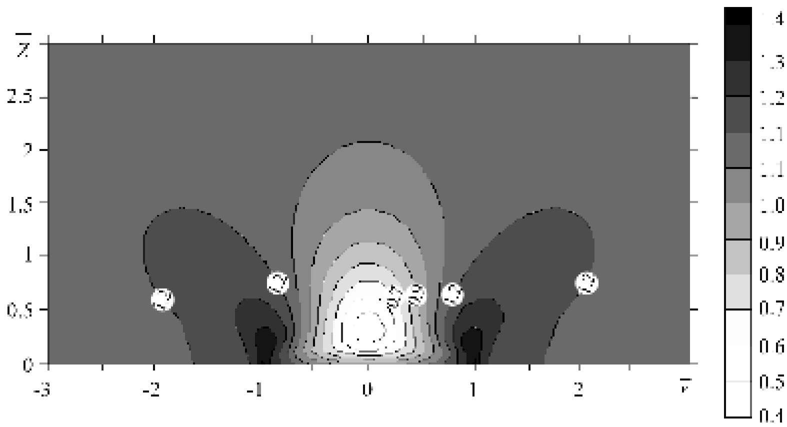

Fig. 7. Maximal shear stress, $10^3 \cdot \bar{\tau}_{max}$.

CONCLUSIONS

The found closed-form solution to the contact problem serves as a theoretical basis for the analysis of strength of the contacting couple with a small surface recess. The analysis has been carried out by utilizing classical fracture criteria, namely the criterion of maximal principle stresses and the criterion of maximal shear stresses.

The cracking of the material of the mated solids can be caused both by compressive and tensile stresses. In a former case the most possible region where the cracks can be initiated is the vicinity of the recess edge. The compressive stresses reach their extreme value at the contact interface at the edge of the recess. On the other hand, due to the defect of geometrical surface structure the tensile stresses within the solids arose. The stresses σ_{rr} and $\sigma_{\theta\theta}$, being tensile in the vicinity of the gap, reach their maximum value at the gap faces, where they are constant and equal to each other. The magnitude of the maximum tensile stress depends on Poisson's ratio of the material and is in the range from 50% to 100% of the applied load at infinity. Two directions of cracking along the radial and circular co-ordinate lines are equally possible.

According to the criterion of the maximal shear stresses the most possible region where plastic zones can be initiated is the vicinity of the recess edge.

РЕЗЮМЕ. Проаналізовано напружено-деформований стан контактної пари з двох ізотропних півбезмежних тіл, одне з яких має малу гладку виїмку. На підставі класичних критеріїв руйнування, а саме, критерію максимальних головних напружень та критерію максимальних дотичних напружень визначено найвірогідніші області зародження тріщин та області появи пластичних зон. Встановлено, що крихке руйнування може бути ініційоване напруженнями розтягу, що виникають в тілах внаслідок поверхневої неоднорідності, а також внаслідок напружень стиску. Для розглянутої у роботі форми виїмки максимальні значення головних напружень та максимальних дотичних напружень досягаються на поверхні контакту, що свідчить про поверхневе руйнування тіл.

РЕЗЮМЕ. Проанализирован напряженно-деформируемое состояние контактной пары из двух изотропных полубесконечных тел, одно из которых имеет локальную гладкую выемку. На основании классических критериев разрушения, а именно, критерии максимальных главных напряжений и максимальных касательных напряжений, определены наиболее вероятные области зарождения трещин и области появления пластичных зон. Установлено, что хрупкое разрушение может быть вызвано как сжимающими напряжениями, так и растягивающими напряжениями, которые возникают вследствие дефекта геометрической поверхностной структуры. Для рассмотренной в работе формы выемки максимальные значения главных напряжений и максимальных касательных напряжений достигаются на поверхности контакта, что свидетельствует о процессе поверхностного разрушения тел.

1. *Monastyrskyy B. and Kaczyński A.* Contact interaction of two elastic half-spaces with a circular recess // Фіз.-хім. механіка матеріалів. – 2010. – **46**, № 3. – P. 47–56.
2. *Johnson K. L.* Contact Mechanics. – Oxford University Press, Oxford: 1985.
3. *Колесников Ю. В., Морозов Е. М.* Механика контактного взаимодействия. – М: Наука, 1989 – 224 с.
4. *Kryshtafovych A. and Martynyak R.* Strength of a system of mated anisotropic half-planes with surface recesses // Int. J. Eng. Sci. – 2001. – **39**. – P. 403–413.
5. *Градштейн И. С., Рыжик И. М.* Таблицы интегралов, сумм, рядов и произведений. – М.: Наука, 1971. – 1108 с.
6. *Прудников А. П., Брычков Ю. Л., Маричев О. И.* Интегралы и ряды. Специальные функции. – М.: Наука, 1983. – 752 с.
7. *Божидарник В. В., Сулим Г. Т.* Елементи теорії пластичності та міцності. Т. І і ІІ. – Львів: Світ, 1999. – І – 532 с.; ІІ – 418 с.

Одержано 27.10.2009